Transcriptional modulator *ZBED6* affects cell cycle and growth of human colorectal cancer cells

Muhammad Akhtar Ali[a,1], Shady Younis[b,c,1], Ola Wallerman[d], Rajesh Gupta[b], Leif Andersson[b,d,e,1,2], and Tobias Sjöblom[a,1]

[a]Science For Life Laboratory, Department of Immunology, Genetics and Pathology, Uppsala University, SE-751 85 Uppsala, Sweden; [b]Science for Life Laboratory, Department of Medical Biochemistry and Microbiology, Uppsala University, SE-751 85 Uppsala, Sweden; [c]Department of Animal Production, Ain Shams University, Shoubra El-Kheima, 11241 Cairo, Egypt; [d]Department of Animal Breeding and Genetics, Swedish University of Agricultural Sciences, SE-75007 Uppsala, Sweden; and [e]Department of Veterinary Integrative Biosciences, College of Veterinary Medicine and Biomedical Sciences, Texas A&M University, College Station, TX 77843

Contributed by Leif Andersson, May 15, 2015 (sent for review December 10, 2014; reviewed by Jan-Ake Gustafsson)

The transcription factor ZBED6 (zinc finger, BED-type containing 6) is a repressor of *IGF2* whose action impacts development, cell proliferation, and growth in placental mammals. In human colorectal cancers, *IGF2* overexpression is mutually exclusive with somatic mutations in PI3K signaling components, providing genetic evidence for a role in the PI3K pathway. To understand the role of *ZBED6* in tumorigenesis, we engineered and validated somatic cell *ZBED6* knock-outs in the human colorectal cancer cell lines RKO and HCT116. Ablation of ZBED6 affected the cell cycle and led to increased growth rate in RKO cells but reduced growth in HCT116 cells. This striking difference was reflected in the transcriptome analyses, which revealed enrichment of cell-cycle–related processes among differentially expressed genes in both cell lines, but the direction of change often differed between the cell lines. ChIP sequencing analyses displayed enrichment of ZBED6 binding at genes up-regulated in *ZBED6*-knockout clones, consistent with the view that ZBED6 modulates gene expression primarily by repressing transcription. Ten differentially expressed genes were identified as putative direct gene targets, and their down-regulation by ZBED6 was validated experimentally. Eight of these genes were linked to the Wnt, Hippo, TGF-β, EGF receptor, or PI3K pathways, all involved in colorectal cancer development. The results of this study show that the effect of ZBED6 on tumor development depends on the genetic background and the transcriptional state of its target genes.

ZBED6 | colorectal cancer | IGF2 | PI3K pathway

Colorectal cancers (CRCs) are caused by sequential mutations in driver genes of key cellular systems such as the Wnt, EGFR/Ras/MAPK, PI3K, TGFB, and TP53 pathways (1). Somatic mutations in the PI3K pathway members *PIK3CA* and *PTEN* occur late in CRC progression and contribute to increased tumor cell growth and invasivity (2–4). In CRC, overexpression of *IGF2* is mutually exclusive with activating genomic alterations of the PI3K pathway genes *PIK3CA* and *PIK3R1* (5). Further, *IRS2* overexpression is mutually exclusive with *IGF2* overexpression. The *IRS2* gene is frequently amplified in CRCs (5) and encodes a protein that links IGF1R, a receptor for IGF1 and IGF2, with PI3K signaling. The importance of this pathway in colorectal tumorigenesis motivates studies to understand its regulation better.

The ZBED6 (zinc finger, BED-type containing 6) transcription factor is a recently discovered negative regulator of IGF2 expression (6, 7). The intronless *ZBED6* gene encodes two N-terminal zinc finger BED domains (8) and an hAT (*hobo*-Ac-Tam3) dimerization domain. Based on its primary structure, *ZBED6* belongs to the hAT transposase family (9). The *ZBED6* gene is located in the first intron of *ZC3H11A* and is transcribed as a composite transcript from the *ZC3H11A* promoter. An SNP (rs4951011) located in the 5′ UTR of *ZBED6* recently was found to be associated with breast cancer susceptibility in a genome-wide association study (10). In pigs, a G-to-A mutation in the highly conserved CpG island in the third intron of *IGF2* was identified as a quantitative trait nucleotide (QTN) with a large impact on body composition (muscle growth and fat deposition); mutant animals showed threefold higher *IGF2* expression in postnatal muscle (11). ZBED6 was identified as the nuclear factor specifically binding the wild-type *IGF2* sequence but not the mutated site. ChIP sequencing (ChIP-seq) in mouse C2C12 cells identified more than 1,200 putative ZBED6 target genes, including 262 genes encoding transcription factors (6). The most common human orthologs of mouse ZBED6 target genes are related to developmental disorders and cancers. *ZBED6* silencing induced *IGF2* overexpression, increased cell proliferation, and accelerated wound healing (6) in C2C12 cells.

The importance of IGF2 and the PI3K pathway activation in cancer, along with the regulatory role of *ZBED6* in IGF2 signaling, prompted us to investigate the role of *ZBED6* in cancer. To explore the interaction between *ZBED6* and its putative target genes in human cells, we knocked out *ZBED6* by homologous recombination in HCT116 and RKO CRC cells. Here we report how this knock-out affects cell growth and gene regulation.

Results

Generation and Validation of *ZBED6* Knockout Cell Lines. The recombinant adeno-associated virus (rAAV) gene-targeting construct was designed to insert a stop codon at position 173 in *ZBED6* by homologous recombination (Fig. 1*A*). We sequentially targeted both *ZBED6* alleles in the human CRC cell lines HCT116 and RKO (Fig. 1*B*) and obtained three independent knockout cell clones for each genetic background. The gene-targeting efficiency

Significance

The *ZBED6* (zinc finger, BED-type containing 6) transcription factor is unique to placental mammals. Its high degree of sequence conservation among placental mammals indicates that it has an essential function. Using two colorectal cancer cell lines we have, for the first time to our knowledge, completely inactivated ZBED6 by genome editing. Our results demonstrate that ZBED6 is not required for cell survival, but its ablation led to consistent changes in cell growth within cell lines but opposite trends between cell lines. The results are in line with the hypothesis that ZBED6 is a transcriptional modulator that does not determine whether or not its target genes are active but fine-tunes their expression. Thus, its effect on tumorigenesis will depend on the transcriptional state of the cell.

Author contributions: L.A. and T.S. designed research; M.A.A., S.Y., O.W., and R.G. performed research; M.A.A., S.Y., O.W., R.G., L.A., and T.S. analyzed data; and M.A.A., S.Y., O.W., L.A., and T.S. wrote the paper.

Reviewers included: J.-A.G., University of Houston.

The authors declare no conflict of interest.

Freely available online through the PNAS open access option.

[1]M.A.A., S.Y., L.A., and T.S. contributed equally to this work.

[2]To whom correspondence should be addressed. Email: leif.andersson@imbim.uu.se.

This article contains supporting information online at www.pnas.org/lookup/suppl/doi:10.1073/pnas.1509193112/-/DCSupplemental.

CELL BIOLOGY

was higher in HCT116 cells (20%) than in RKO cells (1%). Three independent *ZBED6*$^{-/-}$ clones per cell line were selected based on two criteria: complete loss of ZBED6 protein and intact expression of the host gene *ZC3H11A*. In both HCT116 and RKO cell lines, there were no significant changes in *ZC3H11A* mRNA expression between parental cells and *ZBED6*$^{-/-}$ clones (Table S1). However, immunoblot analysis using anti-ZBED6 and anti-ZC3H11A antibodies revealed a complete loss of ZBED6 protein that did not affect the expression of ZC3H11A (Fig. 1*C*). In the parental cells, the *IGF2* expression level was 250-fold higher in HCT116 cells than in RKO cells (Fig. 1*D*, *Left*). In both isogenic models *IGF2* expression was increased in *ZBED6*$^{-/-}$ clones relative to parental cells, 1.4-fold in HCT116 cells and threefold in RKO cells ($P < 0.05$) (Fig. 1*D*, *Right*). Thus, the *ZBED6*$^{-/-}$ knockout cell lines showed loss of ZBED6 expression and retained ZC3H11A expression and up-regulation of *IGF2* expression relative to parental cells, but the relative increase in *IGF2* expression after *ZBED6* silencing differed significantly in the two cell lines (Fig. 1*D*).

Loss of ZBED6 Has Opposite Effects on Cancer Phenotypes in RKO and HCT116 Cells. We assessed the effect of ZBED6 on CRC phenotypes by measuring alterations in growth rate and cell-cycle regulation. Loss of ZBED6 in the three biological replicates of

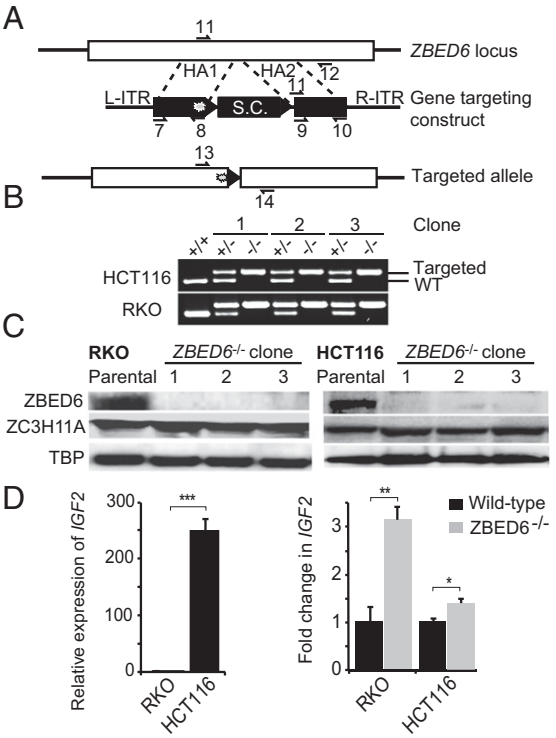

Fig. 1. Knock-out of *ZBED6* in human HCT116 and RKO CRC cells by rAAV-mediated homologous recombination. (*A*) The targeting construct was designed to replace *ZBED6* Q173 by a stop codon. Numbers indicate primers used in HA amplification (7–10), PCR screening (11 and 12), and Cre-mediated removal of the resistance marker (13 and 14) (Table S2). L/R-ITR, left/right inverted terminal repeat; S.C., selection cassette containing neomycin resistance gene; WT, wild-type allele. (*B*) PCR detection of targeted *ZBED6* alleles in parental ($^{+/+}$), heterozygous ($^{+/-}$), and knockout ($^{-/-}$) cells in three independent clones each in HCT116 and RKO cells. The size shift in targeted alleles represents *LoxP* sequences remaining after *Cre*-mediated excision of the resistance marker. (*C*) Immunoblot detection of ZBED6, ZC3H11A, and TBP (loading control) in total cell lysates from parental cells and knockout clones of RKO and HCT116 cell lines. (*D*) RT-PCR analysis of IGF2 expression. (*Left*) Expression level in parental cell lines normalized to RKO. (*Right*) Expression levels in *ZBED6*$^{-/-}$ clones relative to the respective parental cell line.

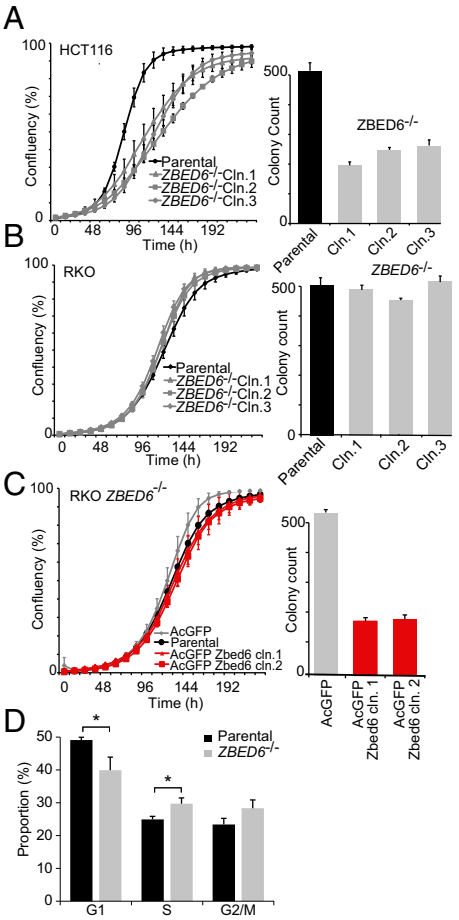

Fig. 2. *ZBED6* ablation alters cell growth in both HCT116 and RKO CRC cells. (*A*) Real-time measurements of cell density (mean ± SD) (*Left*) and clonogenic survival on plastic (*Right*) of 1,000 seeded cells of parental HCT116 cells (black) and *ZBED6*$^{-/-}$ clones (gray). (*B*) Real-time measurements of cell density (mean ± SD) (*Left*) and clonogenic survival on plastic (*Right*) of 1,000 seeded cells of parental RKO cells (black) and *ZBED6*$^{-/-}$ clones (gray). (*C*, *Left*) Real-time measurements of cell density (mean ± SD) for parental RKO cells (black), and *ZBED6*$^{-/-}$ AcGFP (gray) and *ZBED6*$^{-/-}$ AcGFP-Zbed6 (red) clones. (*Right*) Clonogenic survival on plastic of 1,000 seeded *ZBED6*$^{-/-}$ AcGFP clones (gray and *ZBED6*$^{-/-}$ AcGFP-Zbed6 #1 and #2 clones (red). (*D*) Cell-cycle profile of RKO parental cells (black) and *ZBED6*$^{-/-}$ clones (gray).

HCT116 cells had a growth-inhibitory effect and reduced their clonogenic survival (Fig. 2*A*). In contrast, ZBED6 silencing in RKO cells led to a small but consistent increased growth rate but had no significant effect on clonogenic survival (Fig. 2*B*). The heterozygous clones show a growth phenotype similar to their corresponding homozygote knockout clone (Fig. S1).

To verify that the increased growth rate seen in RKO cells indeed was caused by the loss of ZBED6, we performed a rescue experiment in which we stably expressed mouse *Zbed6* in RKO *ZBED6*$^{-/-}$ cells. Two independent clones were obtained, and the expression of full-length Ac*GFP-Zbed6* was confirmed (Fig. S2*A*). The expression of Ac*GFP-Zbed6* was localized to the nucleus (Fig. S2*B*). Although the *ZBED6*$^{-/-}$ clones grew faster than parental RKO cells, Ac*GFP-Zbed6* clones grew at a slower rate than parental RKO and *ZBED6*$^{-/-}$ cells (Fig. 2*C*), and *Zbed6* overexpression reduced clonogenic survival 2.5-fold compared with the RKO *ZBED6*$^{-/-}$ cells (Fig. 2*C*). To understand the underlying reason for the increased growth rate of RKO *ZBED6*$^{-/-}$ cells, we performed cell-cycle analysis and observed a higher fraction of cells in S-phase in RKO *ZBED6*$^{-/-}$ cells than in their parental cells (Fig. 2*D*).

Our attempts to express mouse *Zbed6* stably in HCT116 *ZBED6*$^{-/-}$ cells failed. Our experience and previously published

data (12) indicate that it is more challenging to overexpress ZBED6 stably than to silence this transcript.

Direct and Indirect Effects of *ZBED6* Deletion on the Transcriptome of CRC Cells. We performed whole-transcriptome analyses (RNA-seq) using three independent *ZBED6*$^{-/-}$ clones as biological replicates for both RKO and HCT116 cell lines (Fig. 3*A*). Read alignment with TopHat identified 11,084 genes expressed in RKO cells at sufficient levels for differential expression (DE) analysis using Cufflinks. The expression of 2,807 genes was found to be changed significantly ($P < 0.05$ after Benjamini–Hochberg correction for multiple testing), with 1,310 up-regulated and 1,497 down-regulated genes in the *ZBED6*$^{-/-}$ RKO clones. Principal component and dendrogram analyses separated the respective parental cell line from their *ZBED6*$^{-/-}$ derivatives (Fig. S3). For HCT116, 2,229 of 11,903 expressed genes were identified as DE ($P < 0.05$); 1,378 genes were up-regulated, and 851 genes were down-regulated. Gene ontology (GO) analysis was performed by comparing DE genes with all expressed genes as a background and revealed a significant enrichment of genes related to the regulation of cell proliferation and cell cycle in both RKO and HCT116 cells (Fig. 3*B* and Dataset S1). When the direction of change was taken into account, we found that the most striking enrichment for cell-cycle–related categories such as mitosis and M-phase were associated with up-regulated genes in RKO cells, whereas genes annotated as associated with cell death and negative regulation of cell proliferation tended to be up-regulated in HCT116 cells (Fig. S4*B*). Genes involved in cell proliferation also appeared to be enriched among down-regulated genes in HCT116 cells (Fig. S4 and Dataset S1). These patterns of altered transcription are consistent with the striking difference in phenotypic change after ZBED6 knockout, in which RKO and HCT116 cells show increased and decreased proliferation, respectively. Fig. 3*C* illustrates examples of genes associated with cell proliferation that showed opposite trends in RKO and HCT116 cells after *ZBED6* knock-out.

Most (87.5%) of the genes identified as expressed in HCT116 cells also were expressed in RKO cells. There was a significant overlap of DE genes (χ^2, d.f. = 1, $P < 10^{-4}$), with 608 genes in common. However, there was no consistent direction of DE; only half had the same direction of change in the two cell lines; 194 were up-regulated and 113 were down-regulated in RKO and HCT116 *ZBED6*$^{-/-}$ cells (Fig. S4*A*). The percentage of overlapping genes was slightly higher for the up-regulated genes than for the down-regulated genes (14.9% vs. 12.7%), possibly because of a repressive effect of ZBED6 at a subset of the DE genes, similar to its effect at *IGF2*. To test this notion further, we used ChIP-seq in parental HCT116 cells to identify genes bound by ZBED6 in CRC cells (Fig. S5). This analysis gave more than 7,000 peaks with significant ZBED6 enrichment, with 70% occurring within 1 kb of a refGene transcription start site (TSS). We found ZBED6 sites to be enriched at up-regulated genes compared with down-regulated genes, and this difference was more pronounced when only genes showing DE in the two cell lines were considered (Fig. 3*D*). This enrichment was caused by a larger number of genes with strong ZBED6 enrichment among up-regulated

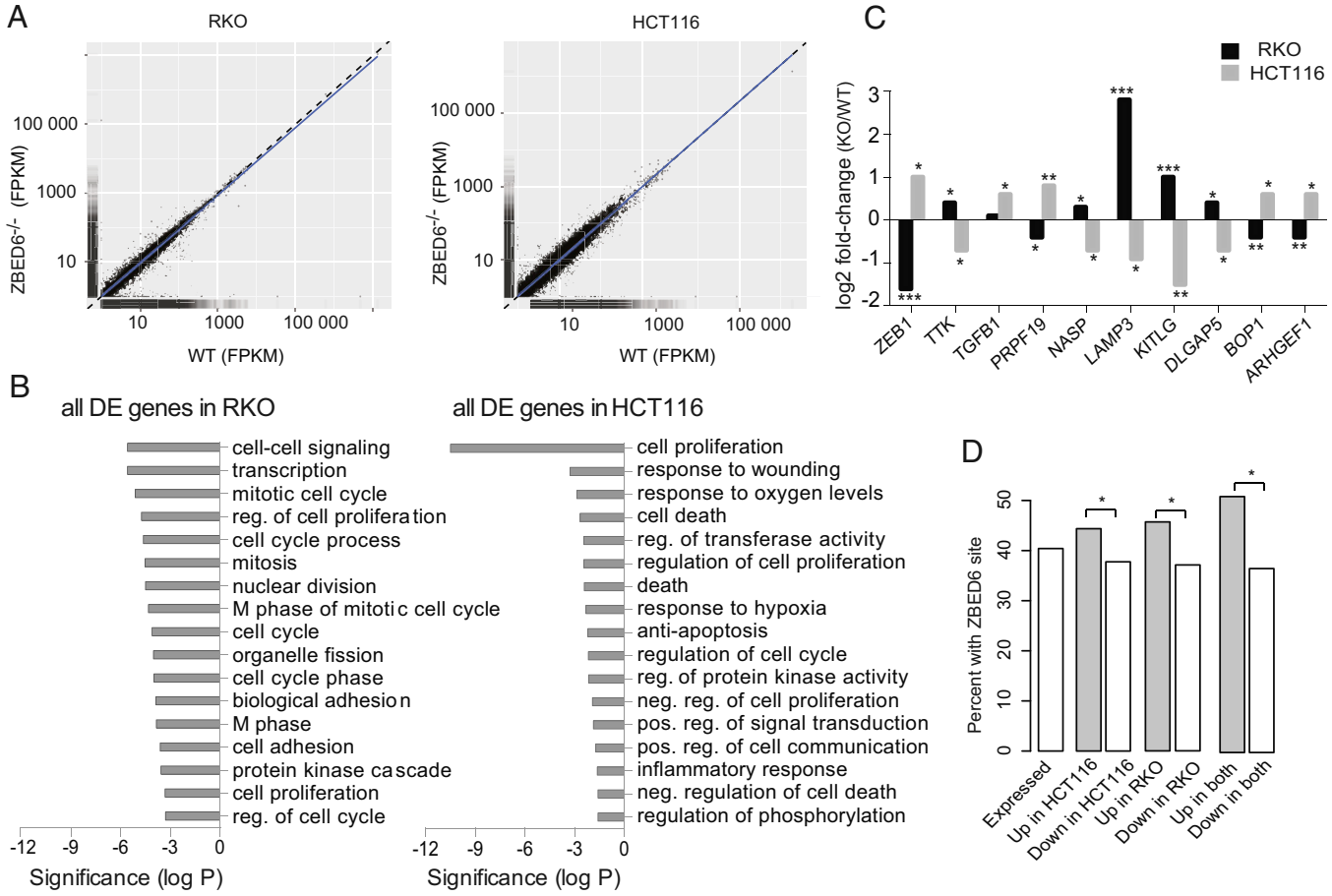

Fig. 3. Transcriptome analysis of RKO and HCT116 parental cells and *ZBED6*$^{-/-}$ *KO* clones. (*A*) Gene expression as FPKM values in parental versus *ZBED6*$^{-/-}$ cells. (*B*) GO analysis of the DE genes. Gray bars represent multiple testing-corrected *P* values for enriched GO categories. (*C*) Fold-change of genes that are associated with cell proliferation and that showed opposite direction of change in RKO and HCT116 cells. *$P < 0.05$; **$P < 0.01$; ***$P < 0.001$. (*D*) ZBED6 sites were enriched at up-regulated genes (gray bars), with the largest difference seen for genes that are up-regulated in both HCT116 and RKO. *$P < 0.05$, Fisher's exact test.

genes, with 16 of the shared up-regulated genes (19%) having a ZBED6 peak with a score above 30 within 1 kb of the TSS, whereas only 4 (7%) of the down-regulated genes had scores exceeding 30 (Table 1). These results suggest that ZBED6 is a direct repressor of several up-regulated genes after ZBED6 silencing.

Validation of Putative Direct ZBED6 Gene Targets. Given the enrichment of ZBED6 peaks at up-regulated genes and the established role of ZBED6 as a repressor of IGF2, we selected for further validation 10 potential direct ZBED6 target genes [*ARL4C, FOSL2, MYBL1, PMEPA1, ROCK2, SGK1, SPTBN1, TCF7, WWC1, WWTR1*) (Table 1)] that (*i*) were up-regulated ≥1.5-fold in both RKO and HCT116 *ZBED6*$^{-/-}$ cells and (*ii*) had a strong ZBED6 ChIP-seq peak near the TSS (Fig. 4*A* and Fig. S5). We evaluated expression change by quantitative PCR (qPCR) in both isogenic pairs and observed significant changes for all these genes in RKO *ZBED6*$^{-/-}$ cells and for the majority of these genes in HCT116 *ZBED6*$^{-/-}$ cells (Fig. 4 *B* and *C*). In parallel, we knocked down the expression of *ZBED6* in HCT116 parental cells using siRNA. Near 50% silencing of *ZBED6* expression was obtained, resulting in alterations in expression similar to those observed in HCT116 *ZBED6*$^{-/-}$ cells with statistically significant up-regulation of six genes (Fig. 4*D*).

Discussion

ZBED6 is unique to placental mammals and has evolved from a DNA transposon that integrated into an intron of *ZC3H11A* in the genome of a common ancestor of all mammals more than 200 million years ago (6, 13). ZBED6 apparently has evolved an essential role, because all placental mammals sequenced so far maintain a well-conserved copy of *ZBED6*, and the two DNA-binding domains show 100% sequence identity across species. Here, for the first time to our knowledge, *ZBED6* has been completely inactivated by genome editing. The expression of *ZC3H11A* was not affected by the genome editing, even though *ZBED6* is located in its first intron (6), but ZBED6 protein expression was abrogated completely. Thus, we can conclude that the phenotypic effects reported here are caused by the ZBED6 knock-down. Our results demonstrate that ZBED6 is not required for cell survival, but its ablation led to consistent changes in cell growth among three biological replicates of the same cell lines. However, the phenotypic consequences of *ZBED6* inactivation were strikingly different in the two cell lines: HCT116 and RKO *ZBED6*$^{-/-}$ cells showed reduced and increased growth, respectively. The similarities in growth phenotypes observed in the heterozygote clones could indicate (*i*) a dominant-negative effect of the targeted allele or (*ii*) haploinsufficiency of *ZBED6*. Although a dominant-negative effect is perhaps less likely, because dimerization is driven by domains C-terminal of the truncating mutation, haploinsufficiency remains a possible explanation. Furthermore, ZBED6 inactivation led to substantial changes in RKO and HCT116 transcriptomes, because the expression of thousands of transcripts was altered significantly. However, the effects on transcriptional regulation also differed considerably between the cell lines, both in the transcripts that showed DE and in the direction of change; only half of the overlapping DE genes had the same direction of change in gene expression. These conflicting changes in phenotypes and transcriptional regulation are consistent with the emerging view that ZBED6 is a transcriptional modulator that does not determine whether other genes are active but that interacts with active promoters and fine-tunes the level of gene expression without recruiting classical silencing mechanisms (14). Thus, we conclude that the effect of *ZBED6* on tumor development depends on the genetic background and the transcriptional state of its target genes.

ZBED6 acts as a repressor of *IGF2* expression in placental mammals as demonstrated in pigs used for meat production (6, 11), in mouse C2C12 cells (14), in mouse pancreatic islet cells (15), and now in human CRC cells. However, the increase in *IGF2* expression after disruption of the binding of ZBED6 to the intronic *IGF2* site in pig skeletal muscle (approximately threefold), in C2C12 cells (approximately twofold), and in CRC cells (1.4- to threefold) is modest compared with the dramatic increase that occurs after differentiation of C2C12 cells (14) or the 250-fold difference in *IGF2* expression between RKO and HCT116 cells. Although IGF2 was barely detectable before ZBED6 removal from RKO cells, the faster-growing HCT116 cells already had high *IGF2* levels. It is possible that IGF2 is not a limiting factor for these cells and therefore the moderate 1.4-fold increase after *ZBED6* silencing had no impact on cell proliferation. In contrast, the threefold increase in *IGF2* expression in RKO cells could have triggered the increased proliferation. Given the successful rescue experiment, we propose that the observed proliferation of RKO cells after ZBED6 ablation is primarily an effect of increased *IGF2* expression. This hypothesis can be tested experimentally by destroying the ZBED6-binding site in *IGF2* in RKO wild-type cells; the hypothesis predicts that the effects on cell proliferation should be similar to those observed in the present study in which *ZBED6* was inactivated. Such an experiment also should shed light on how much of the observed changes in gene expression are secondary effects caused by increased IGF2 signaling.

Transcriptome analyses showed that one-fifth to one-quarter of the expressed genes were differentially expressed in *ZBED6*$^{-/-}$ cells relative to parental HCT116 and RKO cells. Thus, *ZBED6* silencing was associated with substantial changes in the transcriptome, but how many of the DE genes are direct targets for ZBED6 remains an open question. After combining ChIP-seq and gene expression analyses, 10 genes that had ZBED6-binding sites near the TSS and increased expression in *ZBED6*$^{-/-}$ cells were selected as putative direct ZBED6 targets and were validated with qPCR. In qPCR validation experiments, all these genes were up-regulated in RKO and/or HCT116 *ZBED6*$^{-/-}$ cells, and the majority were significantly up-regulated upon siRNA-mediated knock-down of ZBED6 in HCT116 cells. Strikingly, two—*MYBL1* (16) and *SPTBN1* (17, 18)—were bona fide cancer genes, and six genes were linked to pathways involved in CRC: two [*ARL4C* (19) and *TCF7*] to the Wnt pathway, three [*ARL4C* (19), *WWC1*/*KIBRA*

Table 1. Candidate genes for direct ZBED6 targets

Genes	Fold-change		ChIP-seq
	RKO	HCT116	
Up-regulated genes			
SPTBN1	1.53	2.16	421
COL13A1	4.29	2.08	356
WWC1	1.60	2.27	249
WWTR1	1.62	1.52	192
TCF7	2.00	2.25	140
PMEPA1	2.25	11.96	80
ARL4C	2.99	2.69	73
MYBL1	2.01	2.53	69
FOSL2	1.83	1.91	61
ROCK2	1.52	1.73	59
KCTD1	1.54	1.68	54
MAP3K14	1.56	1.74	48
SGK1	1.73	3.25	43
TUBB3	2.75	1.95	42
MB21D2	1.95	2.30	39
CRIM1	3.20	2.39	36
Down-regulated genes			
PPAT	0.60	0.62	300
UPP1	0.04	0.50	62
DDIT4	0.41	0.23	59
ANKRD50	0.29	0.59	33

Genes with at least 1.5-fold change in the same direction in RKO and HCT116 *ZBED6*$^{-/-}$ cells and a ChIP-seq peak with at least 30 reads in HCT116. RNA-seq fold-changes for RKO and HCT116 are given followed by the peak height of the nearest ZBED6 binding site. The 10 genes selected for validations are shown in bold.

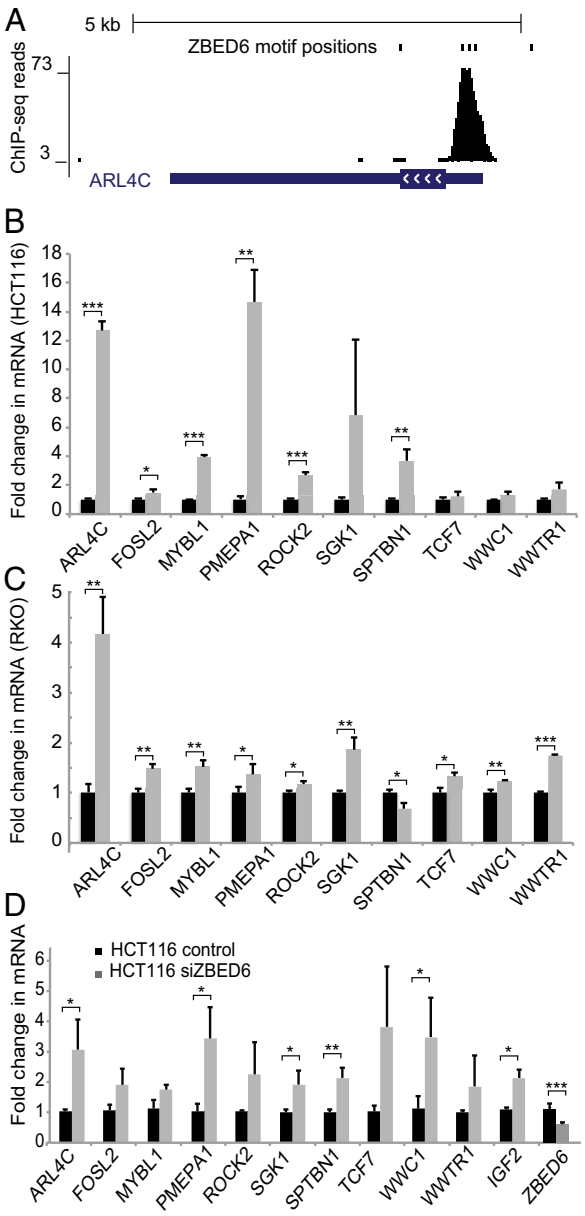

Fig. 4. Validation of 10 genes bound by ZBED6 and up-regulated in *ZBED6*$^{-/-}$ cells. Ten genes up-regulated in both HCT116 and RKO *ZBED6*$^{-/-}$ cells with a ZBED6-binding site near the TSS were selected for validation. (*A*) ChIP-seq enrichment in one of the candidate genes, *ARL4C*. (*B* and *C*) Validation by qPCR of expression change in HCT116 and RKO cells. Black bars represent parental cells; gray bars represent *ZBED6*$^{-/-}$ cells. (*D*) Expression of *ZBED6* and its target genes after siRNA knockdown of ZBED6 measured by qPCR. Error bars indicate SD. $*P < 0.05$; $**P < 0.01$; $***P < 0.001$.

(20), and *WWTR1/TAZ*] to the Hippo pathway, and three [*SPTBN1* (21), *PMEPA1* (22), and *ROCK2* (23)] to the TGF-β pathway. The Hippo pathway is connected by EGFR signaling to the EGFR pathway, which is important for CRC growth, through activation of the Hippo pathway transcription factor Yorkie (24). Thus, apart from its action on *IGF2*, ZBED6 can modulate several pathways essential to CRCs.

In summary, inactivation of *ZBED6* in human CRC cells results in the up-regulation of IGF2 and a subset of other direct targets of ZBED6 in CRC pathways and altered growth of CRC cells. The cell systems provided here open new avenues to study the role of ZBED6 in colorectal tumorigenesis.

Materials and Methods

Gene-Targeting Constructs. To knock out *ZBED6*, a rAAV gene targeting construct was designed (*i*) to mutate Q173 to a stop codon (CAA→TAA), (*ii*) to delete the following nucleotide (A), and (*iii*) to insert a scar sequence (LoxP) containing stop codons in several reading frames to ensure loss of function. The PCR primers used in plasmid construction and integration screening are listed in Table S2. Left and right homology arms (HAs) were amplified from genomic DNA of HCT116 with the left HA containing the Q173 CAA→TAA mutation. Phusion DNA polymerase (Finnzyme) and *attB* tailed primers 1–4 were used to amplify the HAs. The PCR conditions were initial denaturation at 98 °C for 3 min, three cycles of denaturation at 98 °C for 20 s, annealing at 64 °C for 20 s, and extension at 72 °C for 30 s, followed by three cycles at 61 °C and 58 °C annealing temperature, respectively. The final amplification had 25 cycles of denaturation at 98 °C for 20 s, annealing at 57 °C for 20 s, and extension at 72 °C for 30 s. Next, 100 ng each of the HA1 and HA2 PCR products was recombined with 150 ng of pDONR P1-P2 and pDONR P3-P4, respectively, using BP Clonase II (11789-020; Invitrogen) according to the manufacturer's instructions. The resulting entry clones were screened for the presence of HAs by colony PCR amplification using Platinum Taq DNA polymerase (Invitrogen) and M13 primers 5 and 6 flanking the cloned HAs in the pDONR vectors. The products from the colony PCR for pEntry-HA1 were sequenced to ensure the presence of the CAA→TAA mutation in the HA1. Next, 10 fmol of each of pEntry-HA1 (harboring Q173* in HA1), pBUOY.SA.IRES.Neo.pA, and pEntry-HA2 vector were recombined with 15 fmol of the pAAV-Dest vector using LR Clonase II (Invitrogen) according to the manufacturer's instructions. The correct orientation of all three components in the final targeting construct was confirmed by colony PCR using LR screening primers 7–10. The AAV293 packaging cell line (Stratagene) was maintained in DMEM supplemented with 10% FBS and 1% penicillin-streptomycin (Invitrogen) at 37 °C and 5% CO_2. To produce rAAV particles containing single-stranded targeting DNA, 5 μg of each targeting construct, pHelper and pRC (Stratagene), was cotransfected into 80% confluent AAV293 cells in a 75-cm^2 flask using Lipofectamine (Invitrogen). The rAAV particles containing the targeting construct were harvested as crude cellular lysate 48 h after transfection (25).

Knock-Out of ZBED6 in HCT116 and RKO Human CRC Cells. The cell lines HCT116 and RKO were purchased from American Type Tissue Culture Collection. The cells were maintained in McCoy's 5A medium supplemented with 10% FBS and 1% penicillin-streptomycin (Invitrogen) at 37 °C and 5% CO_2. Six million cells were seeded in 75-cm^2 flasks, and after 24 h the rAAV.ZBED6 particles containing lysate were applied directly to the cells in 4 mL of growth medium. Forty-eight hours after infection, the cells were harvested and seeded into twenty 96-well plates in selection medium containing 450 μg/mL and 800 μg/mL of Geneticin (Invitrogen) for HCT116 and RKO cells, respectively, at limiting dilution. The cells were selected for 3 wk, and the resulting clones were screened for site-specific integration of the targeting construct. Each clone was harvested in 25 μL of trypsin, and 5 μL of cell suspension was added to 12 μL of Lyse-N-Go reagent (Thermo Scientific). To screen the clones for site-specific integration, 1 μL of Lyse-N-Go lysate was used in a Platinum Taq DNA polymerase PCR (20 μL) reaction, using primers 11 and 12. The PCR products from positive clones were sequenced to confirm the mutation engineering. Three independent positive clones from the first allele targeting were randomly selected to remove the selection cassette (SA.IRES.Neo.pA) for each cell line. To excise the selection cassette from the targeted allele in positive clones, 0.5 million cells were seeded in 25-cm^2 flasks, and 10^7 pfu of Ad-CMV-Cre-GFP (Vector Biolabs) were added to the growth medium. The cells were incubated for 24 h and then were seeded into 96-well plates at limiting dilution to get single-cell clones (25). The clones were cultured for 3 wk and then were screened for removal of the selection cassette using Lyse-N-Go and primers 13 and 14. The PCR products also were sequenced to confirm the introduction of the Q173X nonsense mutation in the targeted alleles. Three independent heterozygous knockout clones with the selection cassette removed were selected for each cell line. Gene targeting was repeated to knock out the second wild-type allele.

Real-Time PCR Quantification. Total RNA was extracted from RKO and HCT116 cells using the RNeasy Mini kit (Qiagen), and the samples were treated with DNase I. The High Capacity cDNA Reverse Transcription Kit (Applied Biosystems) was used to generate cDNA from the extracted RNA. qPCR analysis was performed in 384-well ABI MicroAmp Optical Reaction Plates on an ABI 7900 real-time PCR instrument (Applied Biosystems). Forward and reverse primers (IDT) for each gene were mixed with SYBR Green Gene Expression Master Mix (Applied Biosystems) in a 10-μL total reaction volume. Primer sequences are listed in Table S2.

Immunoblot Analysis. Cells were washed in PBS and lysed in modified RIPA lysis buffer [50 mM Tris·HCl (pH 8.0), 150 mM sodium chloride, 1% Triton X-100, 1 mM EDTA, 0.5% Sodium deoxycholate, 1% SDS] containing protease inhibitors (Complete Ultra Tablets; Roche). Lysates were vortexed, incubated on ice for 15 min, and centrifuged at 10,000 × *g* for 15 min at 4 °C. The supernatants were transferred into new tubes, and protein concentrations were determined by Bradford assay (Dye Reagent; Bio-Rad). Equal amounts of total lysates were separated by SDS/PAGE gels (4–12%; Bio-Rad) and transferred into PVDF membranes (Millipore). The membrane was blocked in SuperBlock blocking buffer (Thermo Scientific) and incubated overnight at 4 °C with primary ZBED6 (1:1,000) (6), ZC3H11A (1:3,000; Abcam), or TATA binding protein (TBP) (1:5,000; Abcam) antibodies. Thereafter, the membrane was incubated with secondary anti-rabbit IgG or anti-mouse IgG antibodies conjugated to HRP (1:5,000; Cell Signaling). Proteins were visualized and detected by chemiluminescence (Amersham ECL Prime Detection Reagent; GE Healthcare).

RNA Sequencing. Cells were washed in PBS, and total RNA was extracted using the RNeasy Mini kit (QIAGEN). RNA quality and integrity were measured with an RNA6000Nano Bioanalyzer kit (Agilent Technologies). The MicroPoly(A)Purist kit (Ambion) was used to enrich for mRNA. Briefly, 4 μg total RNA in binding buffer was incubated with oligo-dT cellulose at room temperature for 30 min with shaking. Thereafter, the oligo-dT cellulose was washed and spun down, and the mRNA was eluted in RNA Storage Solution. Strand-specific RNA sequencing libraries were generated in triplicate for parental cells and once for each ZBED6$^{-/-}$ clone from HCT116 and RKO cell lines as described previously (26), but without upper size selection. The libraries were sequenced as 100-bp paired-end reads using Illumina HiSeq. Sequence reads were mapped to the reference human genome (hg19) using TopHat 2.0.10 with default parameters. Cuffdiff was used to identify DE genes using a gene model for hg19 downloaded from the University of California, Santa Cruz (UCSC) genome browser, and the abundance of gene expression was calculated as fragments per kilobase of exon per million fragments mapped (FPKM). For GO analysis, the DE genes were submitted to the Database for Annotation, Visualization and Integrated Discovery (DAVID) Bioinformatics Resources 6.7. All expressed genes were used as background, and the GO_BP_FAT table was used to identify enriched GO terms.

ChIP Sequencing. HCT116 cells were cross-linked with 1% formaldehyde for 10 min, and sonicated chromatin from ∼20 × 10^6 cells was used for immunoprecipitation using 2 μg ZBED6 antibody bound to Protein G beads (Dynal). A barcoded Illumina sequencing library was prepared using NEXTflex adaptors (BIOO Scientific) and enzymes from New England Biolabs and KAPA. The library was sequenced using Illumina HiSEq. 2000. The 100-bp single-end reads were aligned to the hg19 assembly using BWA version 0.5.9 at default settings. SAMtools was used to remove alignments with low alignment quality (<10), and the resulting 7.5 million reads were compared with a public HCT116 input control (ENCODE) using the MACS peak caller (version 1.41) to identify enriched peaks and to create wiggle tracks for visualization. The 8,892 called peaks were filtered further to remove peaks in Satellite and rRNA repeats, and a threshold of a minimum score of 8 (>1 rpm) was applied to give a list of 7,175 ZBED6 peaks.

Silencing of ZBED6. Three Silencer Select siRNAs (Ambion) were used to target the *ZBED6* transcript. The sequences of siRNA oligonucleotides are listed in Table S3. The three siRNAs were transfected at a final concentration of 100 μM/mL using Lipofectamine 2000 (Invitrogen). After 48 h of incubation, total RNA was extracted for qPCR quantification as described above. Scrambled siRNA oligonucleotides were used as control.

Generation of *ZBED6* Knockout Clones with Restored Expression of ZBED6. RKO *ZBED6*$^{-/-}$ cells were transfected with an AcGFP-Zbed6 fusion construct (mouse *Zbed6* cloned in AcGFP1C1 vector (catalog no. 632470; Clontech), and pure single-cell expression clones were obtained by flow cytometry. As a control, AcGFP-expressing *ZBED6*$^{-/-}$ RKO cells were generated also. Control and stably transfected cells were lysed as above, separated by SDS/PAGE, and analyzed by immunoblotting using rabbit polyclonal anti-GFP antibody (catalog no. NB600-308; Novus Biologicals).

Phenotypic Analyses. For cell growth measurements, 30,000 parental HCT116 and RKO cells along with three *ZBED6*$^{-/-}$ clones per cell line were seeded in 12-well plates in 10% FBS or 1% FBS, respectively, and were cultured for 13 d with real-time measurement of cell density every 10–12 h using an IncuCyte instrument (Essen Bioscience). To assess clonogenicity, 1,000 cells per well of parental cells, three *ZBED6*$^{-/-}$ clones, and two *ZBED6*$^{-/-}$- *AcGFP-Zbed6* clones were seeded in triplicate in six-well plate wells and cultured in McCoy's 5A medium with 10% FBS for 2 wk. The resulting colonies were stained in methylene blue and counted. Cell-cycle analyses were performed using FxCycle PI/RNase (LifeTechnologies), and cells were analyzed on an LSRII flow cytometer (BD).

ACKNOWLEDGMENTS. This work was supported by Research Grants F06-0050 and RBa08-0114 from the Swedish Foundation for Strategic Research (to T.S.); Grants 2006/2154, 2007/775, and 2012/834 from the Swedish Foundation for Cancer Research (to T.S.); and by grants from the Higher Education Commission of Pakistan (to M.A.A.) and the Swedish Research Council (to L.A.).

1. Vogelstein B, et al. (2013) Cancer genome landscapes. *Science* 339(6127):1546–1558.
2. Samuels Y, et al. (2004) High frequency of mutations of the PIK3CA gene in human cancers. *Science* 304(5670):554.
3. Ericson K, et al. (2010) Genetic inactivation of AKT1, AKT2, and PDPK1 in human colorectal cancer cells clarifies their roles in tumor growth regulation. *Proc Natl Acad Sci USA* 107(6):2598–2603.
4. Samuels Y, et al. (2005) Mutant PIK3CA promotes cell growth and invasion of human cancer cells. *Cancer Cell* 7(6):561–573.
5. Network T; Cancer Genome Atlas Network (2012) Comprehensive molecular characterization of human colon and rectal cancer. *Nature* 487(7407):330–337.
6. Markljung E, et al. (2009) ZBED6, a novel transcription factor derived from a domesticated DNA transposon regulates IGF2 expression and muscle growth. *PLoS Biol* 7(12):e1000256.
7. Lander ES, et al.; International Human Genome Sequencing Consortium (2001) Initial sequencing and analysis of the human genome. *Nature* 409(6822):860–921.
8. Aravind L (2000) The BED finger, a novel DNA-binding domain in chromatin-boundary-element-binding proteins and transposases. *Trends Biochem Sci* 25(9):421–423.
9. Calvi BR, Hong TJ, Findley SD, Gelbart WM (1991) Evidence for a common evolutionary origin of inverted repeat transposons in Drosophila and plants: Hobo, Activator, and Tam3. *Cell* 66(3):465–471.
10. Cai Q, et al.; DRIVE GAME-ON Consortium (2014) Genome-wide association analysis in East Asians identifies breast cancer susceptibility loci at 1q32.1, 5q14.3 and 15q26.1. *Nat Genet* 46(8):886–890.
11. Van Laere AS, et al. (2003) A regulatory mutation in IGF2 causes a major QTL effect on muscle growth in the pig. *Nature* 425(6960):832–836.
12. Butter F, Kappei D, Buchholz F, Vermeulen M, Mann M (2010) A domesticated transposon mediates the effects of a single-nucleotide polymorphism responsible for enhanced muscle growth. *EMBO Rep* 11(4):305–311.
13. Hayward A, Ghazal A, Andersson G, Andersson L, Jern P (2013) ZBED evolution: Repeated utilization of DNA transposons as regulators of diverse host functions. *PLoS ONE* 8(3):e59940.
14. Jiang L, et al. (2014) ZBED6 modulates the transcription of myogenic genes in mouse myoblast cells. *PLoS ONE* 9(4):e94187.
15. Wang X, et al. (2013) Transcription factor ZBED6 affects gene expression, proliferation, and cell death in pancreatic beta cells. *Proc Natl Acad Sci USA* 110(40):15997–16002.
16. Ramkissoon LA, et al. (2013) Genomic analysis of diffuse pediatric low-grade gliomas identifies recurrent oncogenic truncating rearrangements in the transcription factor MYBL1. *Proc Natl Acad Sci USA* 110(20):8188–8193.
17. Gallagher G, Horsman DE, Tsang P, Forrest DL (2008) Fusion of PRKG2 and SPTBN1 to the platelet-derived growth factor receptor beta gene (PDGFRB) in imatinib-responsive atypical myeloproliferative disorders. *Cancer Genet Cytogenet* 181(1):46–51.
18. Grand FH, et al. (2007) A constitutively active SPTBN1-FLT3 fusion in atypical chronic myeloid leukemia is sensitive to tyrosine kinase inhibitors and immunotherapy. *Exp Hematol* 35(11):1723–1727.
19. Matsumoto S, et al. (2014) A combination of Wnt and growth factor signaling induces Arl4c expression to form epithelial tubular structures. *EMBO J* 33(7):702–718.
20. Yu J, et al. (2010) Kibra functions as a tumor suppressor protein that regulates Hippo signaling in conjunction with Merlin and Expanded. *Dev Cell* 18(2):288–299.
21. Tang Y, et al. (2005) Transforming growth factor-beta suppresses nonmetastatic colon cancer through Smad4 and adaptor protein ELF at an early stage of tumorigenesis. *Cancer Res* 65(10):4228–4237.
22. Singha PK, Yeh IT, Venkatachalam MA, Saikumar P (2010) Transforming growth factor-beta (TGF-beta)-inducible gene TMEPAI converts TGF-beta from a tumor suppressor to a tumor promoter in breast cancer. *Cancer Res* 70(15):6377–6383.
23. Cencetti F, et al. (2013) TGFβ1 evokes myoblast apoptotic response via a novel signaling pathway involving S1P4 transactivation upstream of Rho-kinase-2 activation. *FASEB J* 27(11):4532–4546.
24. Reddy BV, Irvine KD (2013) Regulation of Hippo signaling by EGFR-MAPK signaling through Ajuba family proteins. *Dev Cell* 24(5):459–471.
25. Rago C, Vogelstein B, Bunz F (2007) Genetic knockouts and knockins in human somatic cells. *Nat Protoc* 2(11):2734–2746.
26. Zhong S, et al. (2011) High-throughput illumina strand-specific RNA sequencing library preparation. *Cold Spring Harbor Protoc* 2011(8):940–949.